PROCEEDINGS OF SCIENCE

Modeling and understanding radar echos from particle cascades

Krijn D. de Vries[a,*] **and Jannes Loonen, Isha Loudon, Dylan Frikken, Enrique Huesca Santiago, Katie Mulrey, Steven Prohira for the RET Collaboration**
(a complete list of authors can be found at the end of the proceedings)

[a] *Vrije Universiteit Brussel, Dienst ELEM, IIHE, 1050 Brussels, Belgium*
E-mail: krijn.de.vries@vub.be

High-energy in-ice particle cascades can originate from either cosmic-neutrino interactions in the ice medium itself, or cosmic-ray airshowers propagating into a high-altitude ice sheet. After passing through the ice medium, a short-lived ionization trail is left in its wake that can be detected using radar. We present the expected radar signal and discuss its main features. Understanding the detailed signal properties are crucial in the detection and reconstruction of UHE cosmic-rays and neutrinos using the radar echo method.

10th International Workshop on Acoustic and Radio EeV Neutrino Detection Activities (ARENA2024)
11-14 June 2024
The Kavli Institute for Cosmological Physics, Chicago, IL, USA

*Speaker

PoS(ARENA2024)011

1. Introduction

The radar echo technique was recently put forward to probe the > PeV cosmic neutrino flux [1–3]. Its validity was established during the SLAC T-576 beam-test experiment [4, 5]. After this first detection of a radar echo from a high-energy particle cascade ionization trail, the Radar Echo Telescope for Cosmic Rays (RET-CR) was deployed at Summit Station, Greenland to show the in-nature feasibility of the method [6]. Furthermore, several studies have been performed to show the method's capability to probe the > PeV cosmic neutrino flux, providing excellent sensitivities [7].

Currently, two simulation frameworks exist to model the radar echo from a high-energy particle cascade ionization trail. Where RadioScatter in its standard configuration is run in combination with GEANT4 [8] presents a single particle level Monte-Carlo simulation, MARES presents a more deterministic approach based on particle cascade parameterization, integrating over the response of macroscopic O(cm) scale segments. Both approaches are in excellent agreement with each other and experimental observations [9].

In this work, we present our current understanding of the radar echo that is found through the RadioScatter and MARES simulation frameworks. Using a generic geometry, we observe three clear signal features. The strongest response at the transmit frequency is found in the regime of phase coherence. Additionally, clear diffraction signatures are found. Finally, a high-frequency, high-intensity response is found for receivers located at the Cherenkov angle relative to the cascade direction of movement. Here, it should be noted that this is the case for the specific geometry under consideration, and more generic geometries indicate a more complicated situation in which Cherenkov conditions are found to also depend on the relative motion of the cascade with respect to the transmitter. This will be investigated in a future work.

2. Radar scattering from particle cascades

The radar echo problem is finds its solution in the radar range equation,

$$P_r = P_t G_t \frac{\sigma_{RCS}}{4\pi R_c^2} \frac{A_{eff}}{4\pi R_t^2}, \tag{1}$$

with P_r the received power at the antenna, P_t the transmitted power, G_t the transmitter gain towards the direction of the cascade, that has an effective radar scattering cross-section σ_{RCS} and is located at a distance R_c from the transmitter. The reflected signal propagates freely to the receiver antenna located at a distance R_t, having an effective area A_{eff}. Fixing the geometry, the only unknown is the ionization trail radar echo cross-section, that although not implicitly indicated is a function of its orientation relative to both the transmitter and receiver.

In [9] it is shown that the radar echo cross-section for a single free ionization electron is given by,

$$\sigma_{RCS,e^-} = (\omega^2 W)^2 \sigma_{Thomson}, \tag{2}$$

which is composed of the Thomson scattering cross-section $\sigma_{Thomson}$ for an electron in free space, and a damping factor $(\omega^2 W)^2 \approx \frac{\omega^2}{\nu_c^2}$, due to the $\nu_c \approx O(10 - 100)$ THz collision frequency that governs the many (semi)-elastic collisions of the free charge with the ice particles. Taking a typical transmit frequency of $\nu = \omega/(2\pi) \approx 10^8 - 10^9$ Hz, a significant damping is found. This large

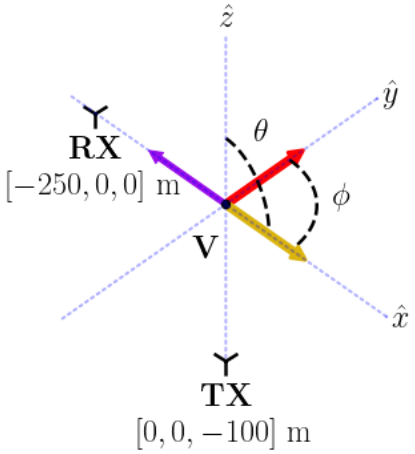

Figure 1: The configuration used to investigate the radar echo signal properties. The cascade is located at the origin and moves in a direction given by the angles θ and ϕ. The transmitter is located at $z = -100$ m below the cascade, and the receiver at $x = -250$ m in the horizontal xy-plane. The three lines correspond to three different cascade directions along the x-axis (yellow, $\theta = 90°$, $\phi = 0°$), the $-x$-axis (purple, $\theta = 90°$, $phi = 180°$), and the y-axis (red, $\theta = 90°$, $\phi = 90°$).

damping factor is compensated by the coherence effect. If the size of the scattering volume is small compared to the other physical dimensions of the system, the cross-section of N particles scales as N^2. A typical particle cascade at PeV energies contains $O(10^{10})$ free charges, with its number scaling linearly with energy, compensating for the collisional losses.

This now allows simulating the scattering of an incoming RF wave off of the ionization trail left in the wake of a high-energy particle cascade using the RadioScatter and MARES simulation frameworks.

3. Signal properties

Given the three-body, transmitter-ionization trail-receiver configuration, it is not possible to cover the full parameter space, but we rather limit ourselves to a single intuitive configuration that is shown in Fig. 1. This now allows us to explore the signal space for cascades moving along a specific (θ, ϕ) direction as seen by the receiver located on the $-x$-axis. This is done modeling a 1 EeV particle cascade, using a transmit frequency of 50 MHz. In Fig. 2, we show the signal amplitude as a function of cascade direction. We see three clear features. First there is the bright, rather wide yellow band of maximum amplitude. Then we also observe diffraction bands, as well as a dark ring. These features are also found on the right-hand side, where we show the frequency at which the maximum amplitude in the Fourier spectrum of the signal is found, where furthermore regions A-D are identified. It is clear that the bright yellow band of maximum amplitude correlates with signals found at the transmit frequency shown by the white band in Fig. 2. The diffraction bands are most prominent in region B, which corresponds to the region in which the cascade is moving away the receiver, and for which a shift to lower frequencies is found. The ring corresponds to the Cherenkov angle, where in this case the amplitude, contrary to expectation, is very weak. On the right-hand

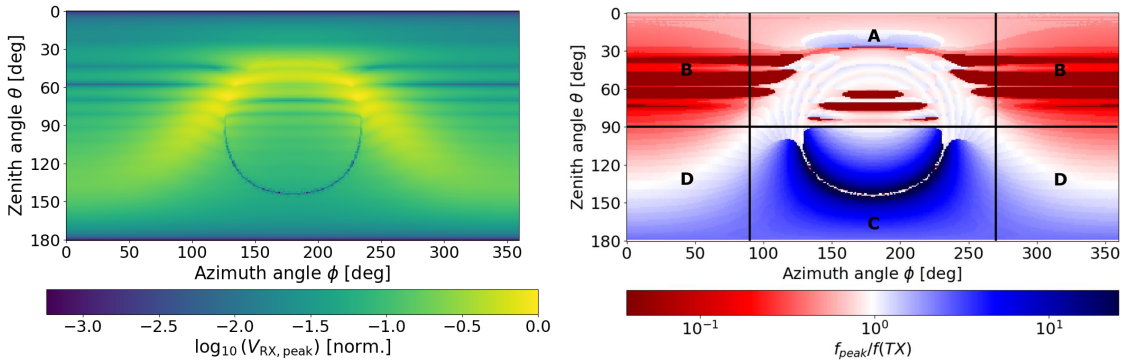

Figure 2: Signal properties for the geometry presented in Fig. 1. The peak amplitude (left) and the maximum amplitude frequency relative to the transmit frequency (right) in which several interesting regions (A-D) are identified.

side, we also see that the frequency content at the Cherenkov angle is strongest at the transmit frequency. This is unexpected, and explained by a simulation effect. At the Cherenkov angle the signal becomes so high-frequency that it was not observed, as in these simulations a sampling frequency of 5 GHz was used. This effect is confirmed by increasing the sampling frequency at the Cherenkov angle in a follow-up study.

Besides the three found features, the right-hand side of Fig 2 labels 4 different geometrical situations that are found to correspond to 4 different frequency shift regions. Region A corresponds to the cascade moving towards the receiver and away from the transmitter, where region D corresponds to its complementary, i.e. the cascade is moving away from the receiver, but toward the transmitter. In these regions, the frequency content is rather complex and moves from low to high frequencies depending on the exact configuration. Regions B and C, however, show a very distinct behavior. In region B, the cascade is moving toward both the receiver and the transmitter, and a clear frequency up-shift is found. Its complementary is found in region C, where the cascade is moving away from both the receiver and the transmitter, for which a clear frequency downshift is found.

One important note to make is that this study was done for the specific geometry under consideration. A first investigation using more generic geometries, for example, already indicate a more complicated situation in which Cherenkov conditions are found to also depend on the relative motion of the cascade with respect to the transmitter, and not only on the reciever. This will be investigated in a future work.

4. Phase coherence

Different features are observed and identified. The main feature is the bright, high-amplitude band at the transmit frequency. To explain this, we need to take a closer look into the concept of phase coherence. As outlined when considering the radar cross-section for multiple particles,

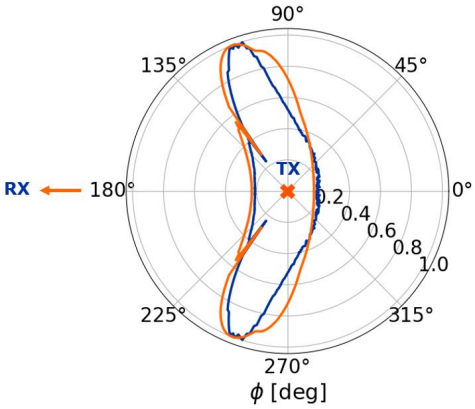

Figure 3: Signal properties for the geometry presented in Fig. 1. The peak amplitude (left) and the maximum amplitude frequency relative to the transmit frequency (right) in which several interesting regions (A-D) are identified.

in case the emission of N individual particles is found to be coherent, the cross-section scales as N^2. The coherence condition was found to be met as long as the spatial dimensions in which the particles were located were much smaller than the typical length scales found in the system. This condition comes forth from the more complete definition of phase alignment. In case the signals from different particles arrive at the receiver with similar phase, they will add coherently. This, more complete definition is relevant in our situation where we consider scattering from the ionization trail left in the wake of a relativistic particle cascade. A measure for phase coherence can be defined as,

$$C = \int \left(\cos(\phi(l)) \frac{n_e^-(l)}{n_{max}} \right)_{t_{max}} dl \tag{3}$$

Here, t_{max} defines the time at which the peak amplitude is observed. At this time, the cosine of the phase ϕ of all particles contributing to the signal is integrated over and normalized. In Fig. 3 we show a polar plot of the normalized peak amplitude, as well as our phase coherence measure. This is done by fixing the zenith angle $\theta = 90^\circ$ and rotating the cascade along its azimuth ϕ. It follows that the phase coherence measure indeed captures all relevant features and provides a good explanation for the observed signal amplitude for the specified geometry. A more complete investigation considering different geometries will be presented in a forthcoming work.

5. Conclusion

We investigated the signal properties of the radar echo off of the ionization trail left in the wake of a high-energy particle cascade. Understanding the detailed signal properties are crucial in the detection and reconstruction of UHE cosmic-rays and neutrinos using the radar echo method. Several features are observed that are linked to diffraction, Doppler and Cherenkov effects, and phase coherence.

References

[1] M. Chiba et al., *Radar for detection of ultra-high-energy neutrinos reacting in a rock salt dome*, *Nucl. Instrum. Meth. A"* **662** (2012) S222.

[2] K.D. de Vries, K. Hanson and T. Meures, *On the feasibility of radar detection of high-energy neutrino-induced showers in ice*, *Astropart. Phys.* **60** (2015) 25.

[3] Radar Echo Telescope collaboration, *The Radar Echo Telescope for Neutrinos*, *PoS* **ICRC2021** (2021) 1195.

[4] S. Prohira et al., *Suggestion of coherent radio reflections from an electron-beam induced particle cascade*, *Phys. Rev. D* **100** (2019) 072003.

[5] S. Prohira, K.D. de Vries, P. Allison, J. Beatty, D. Besson, A. Connolly et al., *Observation of radar echoes from high-energy particle cascades*, *Phys. Rev. Lett.* **124** (2020) 091101.

[6] Radar Echo Telescope collaboration, *The radar echo telescope for cosmic rays: Pathfinder experiment for a next-generation neutrino observatory*, *Phys. Rev. D* **104** (2021) 102006.

[7] Radar Echo Telescope collaboration, *The Radar Echo Telescope*, *PoS* **ARENA2022** (2023) 009.

[8] S. Prohira and D. Besson, *Particle-level model for radar based detection of high-energy neutrino cascades*, *Nucl. Instrum. Methods. Phys. Res. A* **922** (2019) 161.

[9] Radar Echo Telescope collaboration, *Macroscopic approach to the radar echo scatter from high-energy particle cascades*, *Phys. Rev. D* **109** (2024) 083012 [2310.06731].

Full Author List: RET Collaboration (June 28, 2024)

P. Allison[1], J.J. Beatty[1], D.Z. Besson[2], A. Connolly[1], A. Cummings[3,4,5], C. Deaconu[6], S. de Kockere[7], K.D. de Vries[7], D. Frikken[1], C. Hast[8], E. Huesca Santiago[7], C.-Y. Kuo[9], A. Kyriacou[2], U.A. Latif[7], J. Loonen[7], I. Loudon[10], V. Lukic[7], C. McLennan[2], K. Mulrey[10], J. Nam[9], K. Nivedita[10], A. Nozdrina[2], S. Prohira[2], J.P. Ralston[2], M.F.H. Seikh[2], R.S. Stanley[7], J. Stoffels[7], S. Toscano[11], D. Van den Broeck[7], N. van Eijndhoven [7], S. Wissel[4],

[1] Dept. of Physics, Center for Cosmology and AstroParticle Physics, The Ohio State University, Columbus, OH 43210
[2] Dept. of Physics and Astronomy, University of Kansas, Lawrence, KS 66045
[3] Center for Multi-Messenger Astrophysics, Institute for Gravitation and the Cosmos, Pennsylvania State University, University Park, PA 16802
[4] Dept. of Physics, Pennsylvania State University, University Park, PA 16802
[5] Dept. of Astronomy and Astrophysics, Pennsylvania State University, University Park, PA 16802
[6] Dept. of Physics, Enrico Fermi Institue, Kavli Institute for Cosmological Physics, University of Chicago, Chicago, IL 60637
[7] Vrije Universiteit Brussel, HEP@VUB, IIHE, Brussels, Belgium
[8] SLAC National Accelerator Laboratory, Menlo Park, California 94025, USA
[9] Dept. of Physics, Grad. Inst. of Astrophys., Leung Center for Cosmology and Particle Astrophysics, National Taiwan University, Taipei, Taiwan
[10] Department of Astrophysics/IMAPP, Radboud University, P.O. Box 9010, 6500 GL Nijmegen, The Netherlands
[11] Université Libre de Bruxelles, Science Faculty CP230, B-1050 Brussels, Belgium

Acknowledgements

We recognize support from The National Science Foundation under Grants No. 2012980, No. 2012989, No. 2306424, and No. 2019597 and the Office of Polar Programs, the Flemish Foundation for Scientific Research FWO-G085820N, the European Research Council under the European Unions Horizon 2020 research and innovation program (Grant Agreement No. 805486), the Belgian Funds for Scientific Research (FRS-FNRS), IOP, and the John D. and Catherine T. MacArthur Foundation.